Kaleidoscopic Scintillation Event Imaging

Supplementary Material

A. Theoretical Image Truncation Derivation

An event's mirror reflection generated from mirror k is located at $\boldsymbol{p_k}$ with an apparent location at $\boldsymbol{p_k}^{(a)}$. Each edge of the mirror may impose a truncation line on the camera sensor. A truncation line on the sensor, l_{sensor}, is determined as follows. Denote a plane, P_1, that contains $\boldsymbol{p_k}$ and the mirror's edge. If dealing with a second-order reflection or higher, the mirror's edge corresponds to the area where light can arrive on mirror k after being stopped at a previous mirror, which may be different than mirror k's physical edge. Denote the line that intersects P_1 and the scintillator's base surface as l_1. Compute the plane, P_{trunc}, that contains l_1 and $\boldsymbol{p_k}^{(a)}$. Denote the side of P_{trunc} that faces away from the mirror using the normal vector $\boldsymbol{n}_{\text{trunc}}$. Compute the intersection between P_{trunc} and the focal plane to be the truncation line at the focal plane, l_{focal}. Project $\boldsymbol{n}_{\text{trunc}}$ onto the focal plane, denoted as $\boldsymbol{n}_{\text{focal}}$. Scale l_{focal} by the magnification, $m = -\frac{S_2}{S_1}$, to obtain l_{sensor}. Scale $\boldsymbol{n}_{\text{focal}}$ by m to obtain $\boldsymbol{n}_{\text{sensor}}$.

The truncation side of l_{sensor} where photons do not arrive depends on which side of the focal plane that $\boldsymbol{p_k}^{(a)}$ is located. If $\boldsymbol{p_k}^{(a)}$ is beyond the focal plane away from the lens at a distance greater than S_1 from the lens, then the side of l_{sensor} pointed to by $\boldsymbol{n}_{\text{sensor}}$ is truncated and contains no photon arrivals (Fig. 6b). If $\boldsymbol{p_k}^{(a)}$ is between the focal plane and lens at a distance less than S_1 from the lens, then the side of l_{sensor} opposite of $\boldsymbol{n}_{\text{sensor}}$ is truncated and contains no photon arrivals (Fig. 6d).

The area on the sensor where photons cannot arrive is the union of the truncation sides of each truncation line. We denote this area as the "truncation zone" and its complement as the "acceptance zone" (Fig. 6b). The event itself has no truncation zone on the sensor because its image is formed by light emitted directly to the camera without reflections.

B. Imaging Theory Simulation Details

Fig. 3 in the main paper is generated with the following configuration using ray tracing and a thin lens. The simulated scintillator has a 5.77 mm height, 20 mm base length, 120 degree opening angle, and index of refraction $n = 1.5$. A thin lens with 35 mm focal length and 25 mm diameter is placed at $S_1 = 45$ mm away from the focal plane at the scintillator's apex's apparent location. A 512×512 sensor with 18.6 μm pixel pitch is placed at $S_2 = 157.5$ mm away from the lens. 100,000 photons are emitted isotropically from $(-0.5, 0.75, 1)$ mm (world coordinates).

C. Gaussian Mixture Model Formulation

The complete-data likelihood function, L, for an image with N photons, one event, and K mirror reflections is

$$L(\boldsymbol{\theta}; \boldsymbol{t}, \boldsymbol{z}) = \prod_{i=1}^{N} \prod_{k=0}^{K} \left[\pi_k \mathcal{N}(\boldsymbol{t_i}; \boldsymbol{\mu_k}, \sigma_k^2)\right]^{\mathbb{1}(z_i=k)} \tag{9}$$

where $\boldsymbol{\theta} = (\boldsymbol{\mu}, \boldsymbol{\sigma}, \boldsymbol{\pi})$ are model parameters, and π_k is the mixing weight for component k. $\boldsymbol{t} = (\boldsymbol{t_1}, \boldsymbol{t_2}, ..., \boldsymbol{t_N})$ are the 2D coordinates of each of N photon arrivals on the sensor and $\boldsymbol{z} = (z_1, z_2, ..., z_N)$ are the latent variables for which component a photon belongs to. We apply a density-based weighting scheme to photon samples to minimize the influence of sparsely distributed dark counts. The weighted complete-data likelihood function is

$$L_w(\boldsymbol{\theta}; \boldsymbol{t}, \boldsymbol{z}) = \prod_{i=1}^{N} \prod_{k=0}^{K} \left[\pi_k \mathcal{N}(\boldsymbol{t_i}; \boldsymbol{\mu_k}, \frac{1}{w_i}\sigma_k^2)\right]^{\mathbb{1}(z_i=k)} \tag{10}$$

$$= \prod_{i=1}^{N} \prod_{k=0}^{K} \left[\pi_k \frac{w_i}{2\pi {\sigma_k}^2} \exp\left(-\frac{w_i}{2{\sigma_k}^2} ||\boldsymbol{t_i} - \boldsymbol{\mu_k}||_2^2\right)\right]^{\mathbb{1}(z_i=k)}$$

where

$$w_i = \sum_{j \in S_i^q} \exp\left(-\frac{||\boldsymbol{t_i} - \boldsymbol{t_j}||_2^2}{\nu}\right) \tag{11}$$

is the weight assigned to photon i, S_i^q is the set of q nearest neighbors of photon i, and ν is a positive scalar. The expected value of the weighted complete-data log-likelihood, Q, is

$$Q = E_{\boldsymbol{z}|\boldsymbol{t}}\left[\log L_w(\boldsymbol{\theta}; \boldsymbol{t}, \boldsymbol{z})\right] \tag{12}$$

$$= \sum_i \sum_k r_{ik} \Bigg[\log(\pi_k) + \log(w_i) - \log(2\pi {\sigma_k}^2) - \frac{w_i}{2{\sigma_k}^2} ||\boldsymbol{t_i} - \boldsymbol{\mu_k}||_2^2\Bigg]$$

where

$$r_{ik} = E_{\boldsymbol{z}|\boldsymbol{t}}[\mathbb{1}(z_i = k)] = \frac{\pi_k \mathcal{N}(\boldsymbol{t_i}; \boldsymbol{\mu_k}, \sigma_k^2)}{\sum_{k'=0}^{K} \pi_{k'} \mathcal{N}(\boldsymbol{t_i}; \boldsymbol{\mu_{k'}}, \sigma_{k'}^2)} \tag{13}$$

gives the posterior distribution of $\boldsymbol{z}$. r_{ik} is the probability that photon i comes from component k, given the current parameter values.

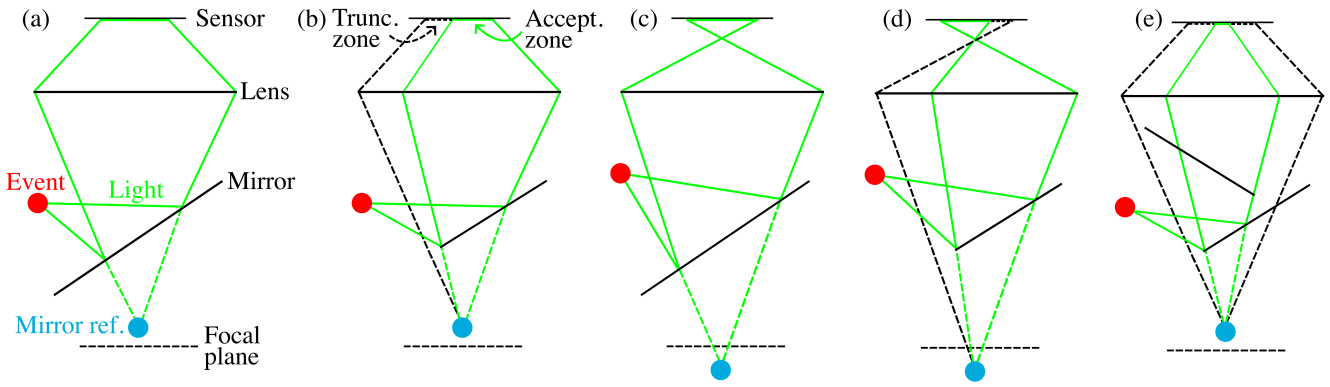

Figure 6. **Mirror apertures and image truncations.** An event emits light onto a mirror that reflects into the camera. Some light from a mirror reflection cannot reach the sensor due to finite mirrors and defocus blur, forming a "truncation zone" on the sensor. The "acceptance zone" denotes the area where light from a mirror reflection can arrive on the sensor. Example cases include the following: The mirror reflection is located within the focal plane (a,b,e) or beyond the focal plane (c,d). All light that forms the mirror reflection reaches the sensor (a,c). Some light that would form the mirror reflection is stopped at the mirror's edge and truncated on the sensor (b,d). Some light that would form a second-order mirror reflection is stopped at both mirrors' edges and truncated on the sensor (e). The mirror for the second reflection in (e) is illustrated along the light's path. Illustrations are drawn with scintillator index of refraction $n = 1$.

D. Experimental Parameter Values

In all experiments, we use the regularization term with $\lambda = 10$. We use $q = 10$ nearest neighbors and $\nu = 10$ pixels for assigning photon weights. Up to ten possible event locations in the scintillator are evaluated in the initialization procedure equispaced over the scintillator's depth. During one M-step, we run gradient ascent for 1,000 steps with a step size of 1e-7. We run the EM algorithm until the distance in the estimated event location between consecutive steps is less than 0.01 mm, or until 100 steps are taken. We clip all σ_k's to a a minimum value of 10 pixels to account for imperfect focusing and a non-ideal point source. The gradient of σ_k is set to 0 if σ_k gets clipped to the minimum value. We set $A = 41.7$ mm, $S_1 = 45$ mm, $S_2 = 72$ mm, and $a = 0.25$. See Appendix E for how we calibrate these camera parameters. The focal plane is set to the scintillator's apparent depth at $z_w = 2.75$ mm.

E. Experimental Camera Parameter Calibration

We select the experimental image shown in Fig. 12 where the event is approximately centered and mirror reflections are near the image's edges. The camera's field of view covers about 5.5 mm at the focal plane, and the $+x$ mirror reflection's photon cluster is approximately centered at pixel coordinate $(470, 256)$. We approximate the observed mirror reflection's x-coordinate in world coordinates as $470/512 \times 5.5/2 = 2.52$ mm. We assign the event's location to be $(0, 0, 2.9)$ mm. This event location and the scintillator's geometry produce a $+x$ mirror reflection located at $x = 2.52$ mm, matching the observed mirror reflection. The event location is fixed, and the camera aperture diameter is set to $A = 50/1.2 = 41.7$ mm. The camera parameter values for S_1, S_2, and a are manually adjusted until the resulting Gaussian components ($\boldsymbol{\mu_k}$,σ_k) coincide with the event and mirror reflection photon clusters. Values are set so that approximately all photons in the photon cluster are contained within a radius of $2\sigma_k$ from component k's centroid (plotted in Fig. 12). Dark counts are ignored. The resulting values are $S_1 = 45$ mm, $S_2 = 72$ mm, and $a = 0.25$. The focal plane is set to the scintillator's apparent depth at $z_w = 5.77 - 5.77/1.91 = 2.75$ mm. The lens plane is set at $z_w = 2.75 + 45 = 47.75$ mm. The sensor plane is set at $z_w = 47.75 + 72 = 119.75$ mm.

F. Ablation Study: Regularization

We perform the same experiments as in Sec. 5 of the main paper on the same 4,379 experimental images containing at least 60 counts, except we set $\lambda = 0$ (no regularization). The results are reported in Figs. 7 and 8. An elevated frequency of images where no photons are removed during mirror reflection removals is observed in Fig. 7. For these images, the algorithm is likely converging to an event location with an erroneously high z_w coordinate. This results in a Gaussian component with a large σ_0 that covers photon clusters of multiple mirror reflections, as shown in Fig. 11a. The high frequency of short distances in Fig. 8 also indicates that mirror reflections are not being properly identified and removed, and the algorithm is converging to the same estimate over multiple identical images. Thus, we observe a decrease in localization performance without regularization.

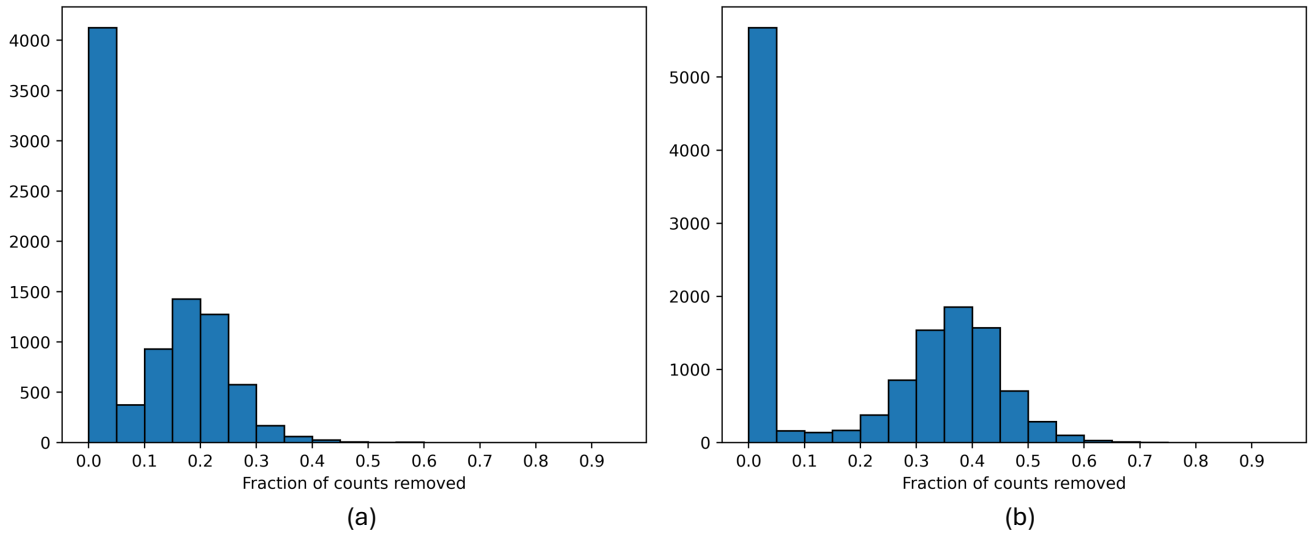

Figure 7. **Ablation study. Experimental fraction of counts in an image removed during mirror removals without regularization ($\lambda = 0$).** (a) One mirror reflection removal. Median, mean, stdev: 0.10, 0.10, and 0.11. 8,972 images. (b) Two mirror reflection removals. Median, mean, stdev: 0.27, 0.21, and 0.19. 13,458 images.

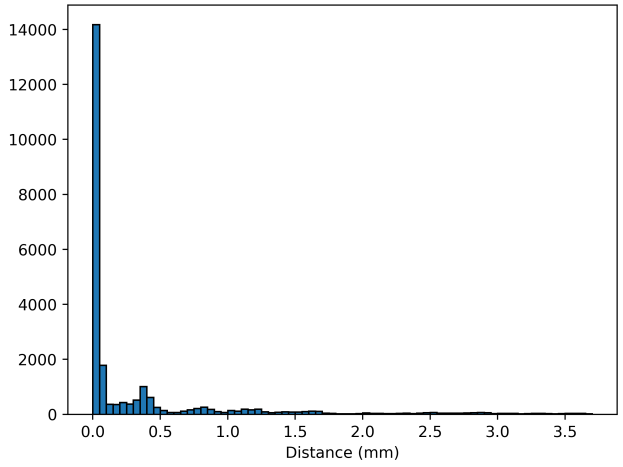

Figure 8. **Ablation study. Experimental agreement in event location measurements without regularization ($\lambda = 0$).** Histogram of distances between mean estimated event location and each image's estimated event location after mirror reflection removals. Median, mean, stdev: 0.03 mm, 0.39 mm, and 0.79 mm. 24,673 distances.

G. Denoising and Estimating Depth from Defocus (Prior Method)

Prior methods that estimate a 3D event location using depth from defocus have also attempted to remove dark counts using a denoising algorithm before solving for the location's maximum likelihood estimate [8]. The denoising algorithm consists of computing the minimum spanning tree among all photons in an image and removing edges longer than a chosen threshold, T_{edge}. The photons in the largest connected component by cardinality are classified as the scintillation photons, and the rest are discarded as dark counts. We test this method on the simulated non-kaleidoscopic images (described in Sec. 6 of the main paper) and report results in Tab. 2. We observe similar performance as the non-kaleidoscopic version of our proposed algorithm.

		Average error and resolution (mm) ↓			
N_0	T_{edge} (pixels)	3D Error	x Res.	y Res.	z Res.
30	40	0.81	1.43	1.41	1.42
	80	0.64	1.04	1.02	1.04
	120	1.26	1.72	1.91	1.73
20	40	0.92	1.59	1.56	1.56
	80	0.68	1.05	1.03	1.06
	120	1.59	2.10	2.38	2.21
10	40	1.14	1.89	1.85	1.90
	80	0.80	1.20	1.13	1.14
	120	2.04	2.84	2.90	2.83

Table 2. **Prior method all simulation results.** Estimating depth from defocus on non-kaleidoscopic images after attempting to remove dark counts as in a prior method [8].

H. Additional Figures

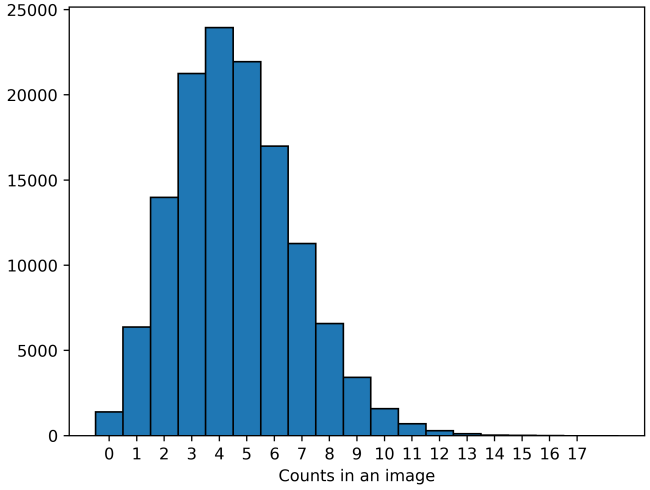

Figure 9. **Histogram of dark counts per experimental image.** A median of 4 dark counts per image after zeroing hot pixels is observed out of 130,000 images taken in the dark with no gamma-ray source present.

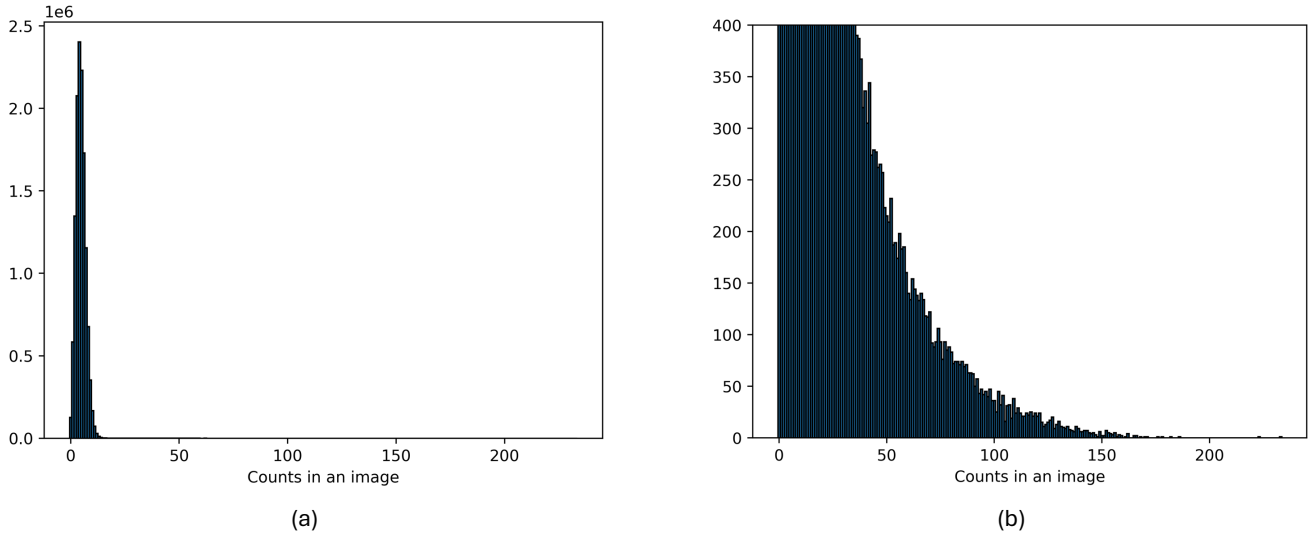

Figure 10. **Histogram of counts per experimental image with the gamma-ray source present.** A median of 4 counts per image after zeroing hot pixels is observed out of 13,000,000 images taken with the gamma-ray source present. a) The full histogram. b) The histogram clipped in the y-axis.

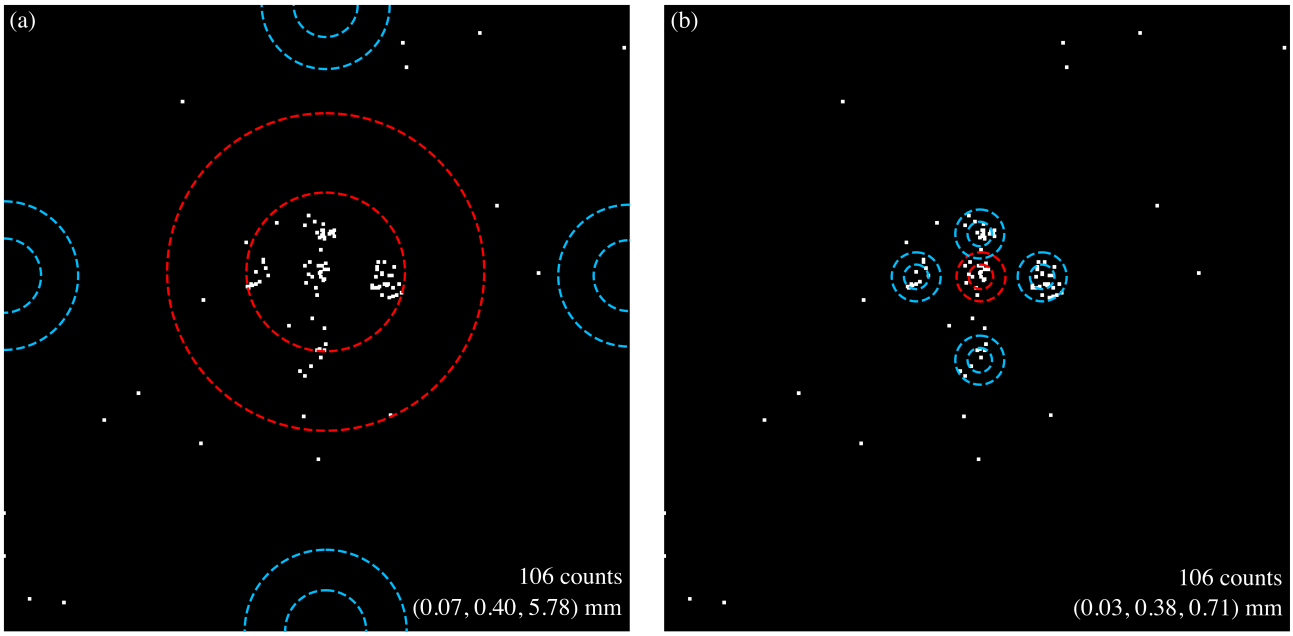

Figure 11. **Regularization example.** An experimental image overlaid with the algorithm's estimated Gaussian components with (a) $\lambda = 0$ (no regularization) and (b) $\lambda = 10$ (regularization). Each dashed red circle is centered on the Gaussian component's mean. The inner and outer circles are one and two standard deviations in radius, respectively. Red and blue circles represent the event and mirror reflections, respectively. The number of counts in the image and the algorithm's estimated event location are shown in each image. Pixels with a photon are enlarged with a 3×3 filter for visualization purposes.

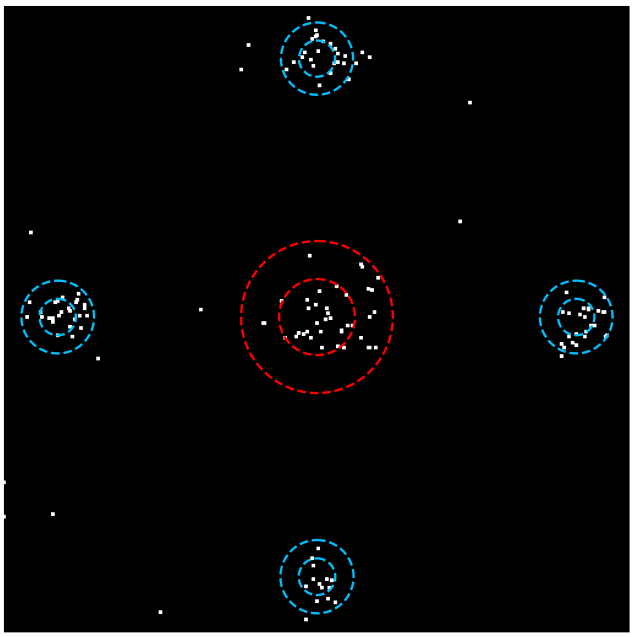

Figure 12. **Selected experimental calibration image.** The image is overlaid with the Gaussian components found after manually adjusting the camera parameters. Each dashed red circle is centered on the Gaussian component's mean. The inner and outer circles are one and two standard deviations in radius, respectively. Red and blue circles represent the event and mirror reflections, respectively. Pixels with a photon are enlarged with a 3×3 filter for visualization purposes.

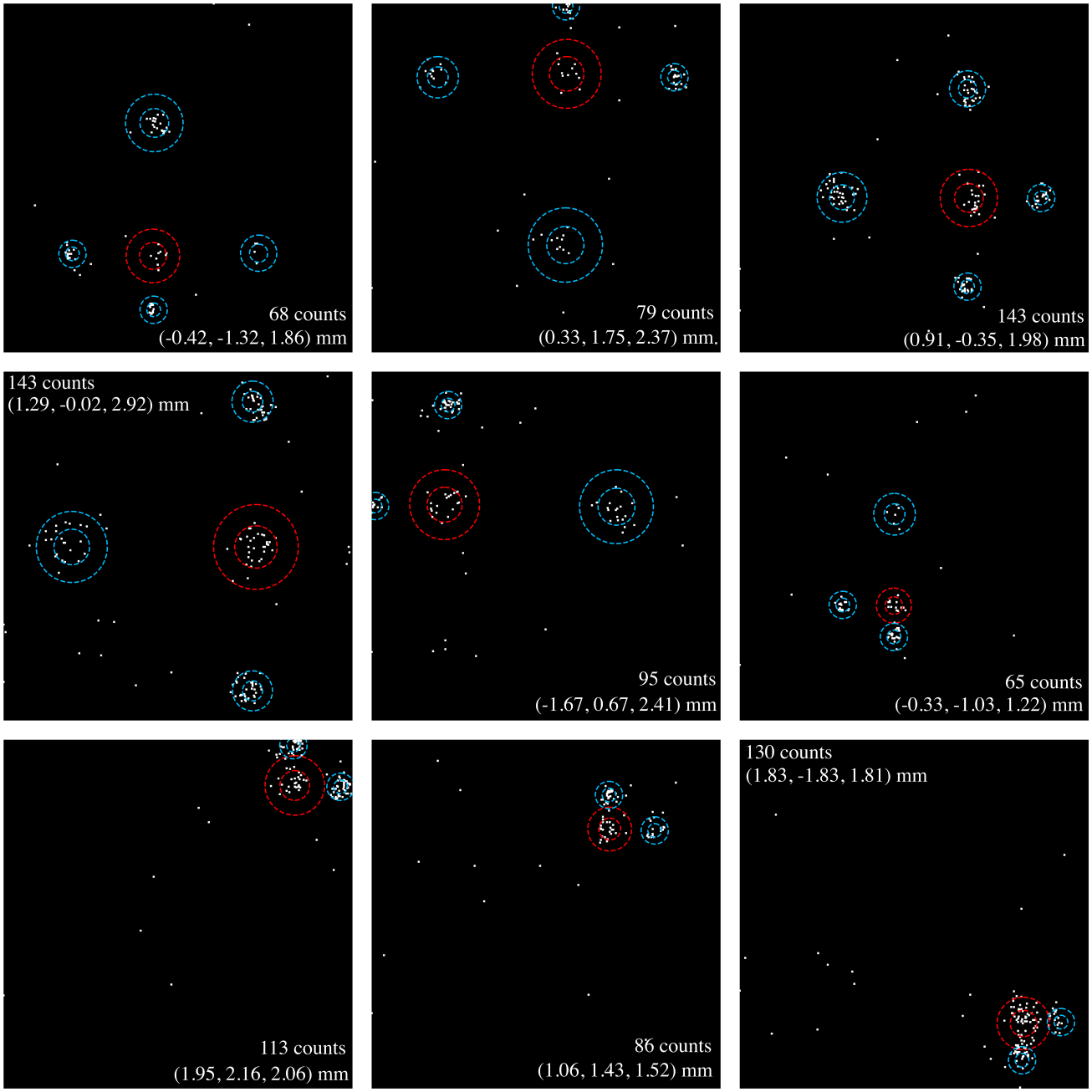

Figure 13. **Additional selected experimental images.** Experimental images overlaid with the algorithm's estimated Gaussian components. Each dashed red circle is centered on the Gaussian component's mean. The inner and outer circles are one and two standard deviations in radius, respectively. Red and blue circles represent the event and mirror reflections, respectively. Pixels with a photon are enlarged with a 3×3 filter for visualization purposes. The number of counts in the image and the algorithm's estimated event location are shown in each image.

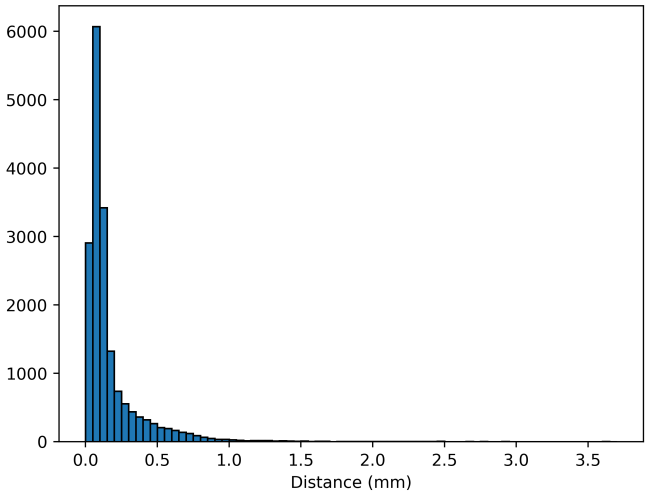

Figure 14. **Experimental agreement in event location measurements using regularization ($\lambda = 10$).** Histogram of distances between mean estimated event location and each image's estimated event location after mirror reflection removals. Median, mean, stdev: 0.10 mm, 0.17 mm, and 0.22 mm. 17,666 distances.

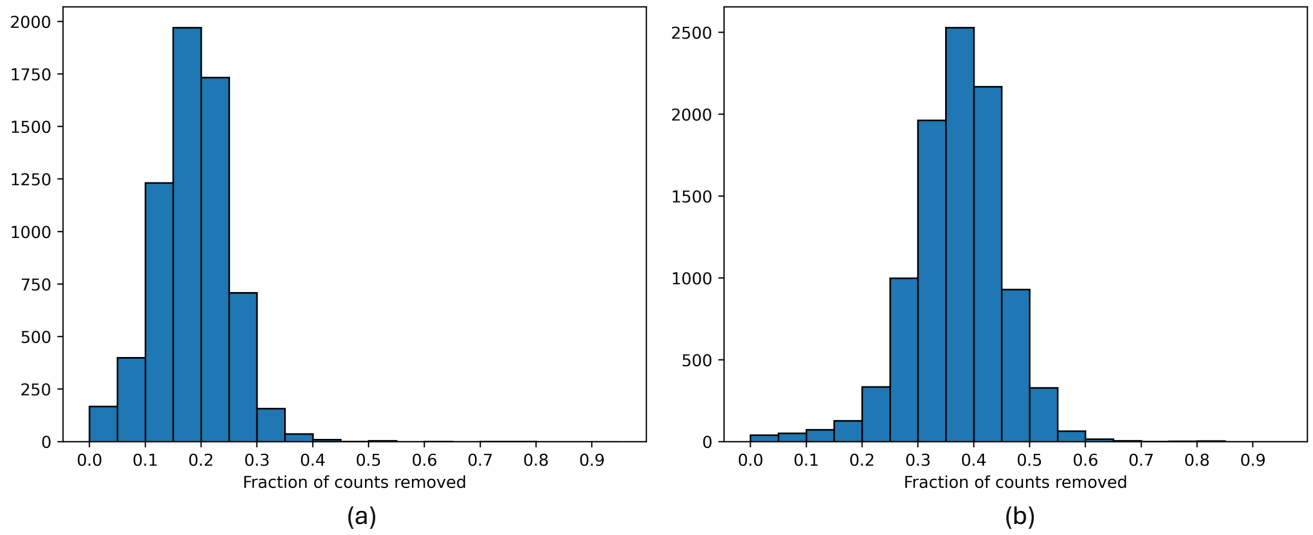

Figure 15. **Experimental fraction of counts in an image removed during mirror removals using regularization ($\lambda = 10$).** (a) One mirror reflection removal. Median, mean, stdev: 0.19, 0.18, and 0.07. 6,424 images. (b) Two mirror reflection removals. Median, mean, stdev: 0.38, 0.37, and 0.08. 9,636 images.

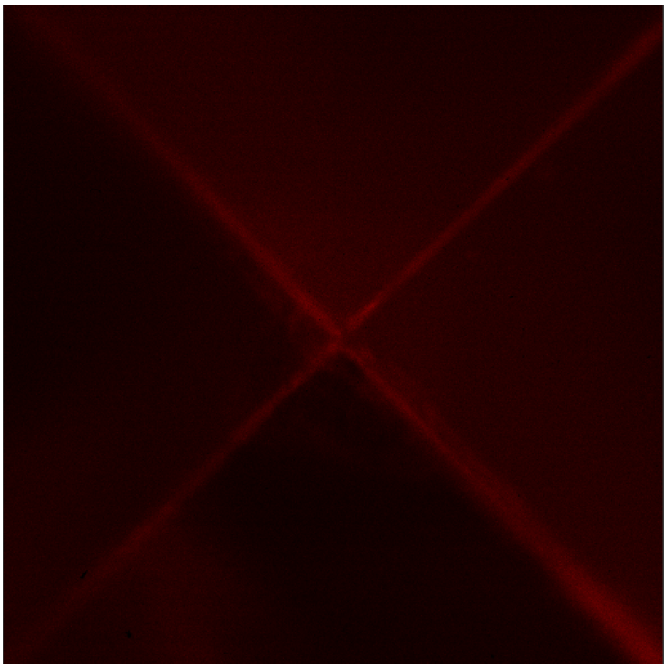

Figure 16. **Experimental focus.** A view of how the camera is focused on the scintillator in the experiments. The edges between mirrors are visible.

I. Gradient Derivations

Consider a square pyramid kaleidoscopic scintillator with height h and index of refraction n. The camera's focal plane is located at the apparent depth of the scintillator's apex at $z_w = h - h/n$ (world coordinates). Denote an event's real location $\boldsymbol{p_0}$ at (x_0, y_0, z_{w0}) in world coordinates. To transform from world coordinates (origin at pyramid apex) to camera coordinates (origin at lens), apply $z_c = z_{lens} - z_w$, where z_{lens} is in world coordinates. The event's mirror reflection k is located at $\boldsymbol{p_k} = (x_k, y_k, z_k) = \boldsymbol{T_k p_0}$. α_{xyk} denotes the coefficient in $\boldsymbol{T_k}$ corresponding to x_0 and y_k. $k = 0$ refers to the event itself, and not a mirror reflection. These derivations assume $\boldsymbol{\mu_k} = \left[\frac{S_2}{z_k}x_k, \frac{S_2}{z_k}y_k\right]$. In these derivations, we use camera coordinates (origin at lens) denoted as z_k instead of z_{ck} as in the main paper. The camera sees events and mirror reflections at their apparent depth rather than their real depth. z_{w0} is the z-coordinate of the event's real location in world coordinates, and z_k is the event or mirror reflection's apparent z-coordinate in camera coordinates.

I.1. Unweighted Likelihood

$$x_k = \alpha_{xxk}x_0 + \alpha_{xyk}y_0 + \alpha_{xzk}z_{w0} \tag{14}$$

$$y_k = \alpha_{yxk}x_0 + \alpha_{yyk}y_0 + \alpha_{yzk}z_{w0} \tag{15}$$

$$z_k = z_{\text{lens}} - \left(h - \frac{h - (\alpha_{zxk}x_0 + \alpha_{zyk}y_0 + \alpha_{zzk}z_{w0})}{n}\right) \tag{16}$$

$$\boldsymbol{\mu_k} = \left[\frac{S_2}{z_k}x_k, \frac{S_2}{z_k}y_k\right] \tag{17}$$

$$\sigma_k = a\frac{AS_2}{S_1}\frac{|S_1 - z_k|}{z_k} \tag{18}$$

$$L(\boldsymbol{\theta}; \boldsymbol{t}, \boldsymbol{z}) = \prod_{i=1}^{N}\prod_{k=0}^{K}\left[\pi_k \mathcal{N}(\boldsymbol{t_i}; \boldsymbol{\mu_k}, \sigma_k^2)\right]^{\mathbb{1}(z_i=k)} \tag{19}$$

$$= \prod_{i=1}^{N}\prod_{k=0}^{K}\left[\pi_k \frac{1}{2\pi{\sigma_k}^2}\exp\left(-\frac{1}{2{\sigma_k}^2}(\boldsymbol{t_i} - \boldsymbol{\mu_k})^T(\boldsymbol{t_i} - \boldsymbol{\mu_k})\right)\right]^{\mathbb{1}(z_i=k)} \tag{20}$$

$$(\boldsymbol{t_i} - \boldsymbol{\mu_k})^T(\boldsymbol{t_i} - \boldsymbol{\mu_k}) = {t_{ix}}^2 - 2t_{ix}\left(S_2\frac{x_k}{z_k}\right) + \left(S_2\frac{x_k}{z_k}\right)^2 + {t_{iy}}^2 - 2t_{iy}\left(S_2\frac{y_k}{z_k}\right) + \left(S_2\frac{y_k}{z_k}\right)^2 \tag{21}$$

$$= {t_{ix}}^2 - 2t_{ix}S_2\frac{x_k}{z_k} + {S_2}^2\left(\frac{x_k}{z_k}\right)^2 + {t_{iy}}^2 - 2t_{iy}S_2\frac{y_k}{z_k} + {S_2}^2\left(\frac{y_k}{z_k}\right)^2 \tag{22}$$

$$Q = \sum_i\sum_k r_{ik}\left[\log\pi_k - \log(2\pi{\sigma_k}^2) - \frac{{\sigma_k}^{-2}}{2}(\boldsymbol{t_i} - \boldsymbol{\mu_k})^T(\boldsymbol{t_i} - \boldsymbol{\mu_k})\right] \tag{23}$$

$$\frac{x_k}{z_k} = \frac{\alpha_{xxk}x_0 + \alpha_{xyk}y_0 + \alpha_{xzk}z_{w0}}{z_{\text{lens}} - \left(h - \frac{h - (\alpha_{zxk}x_0 + \alpha_{zyk}y_0 + \alpha_{zzk}z_{w0})}{n}\right)} \tag{24}$$

$$\frac{y_k}{z_k} = \frac{\alpha_{yxk}x_0 + \alpha_{yyk}y_0 + \alpha_{yzk}z_{w0}}{z_{\text{lens}} - \left(h - \frac{h - (\alpha_{zxk}x_0 + \alpha_{zyk}y_0 + \alpha_{zzk}z_{w0})}{n}\right)} \tag{25}$$

$u_x = x_k = \alpha_{xxk} x_0 + \alpha_{xyk} y_0 + \alpha_{xzk} z_{w0}$
$u_x{}'(x_0) = \alpha_{xxk}$
$u_x{}'(y_0) = \alpha_{xyk}$
$u_x{}'(z_{w0}) = \alpha_{xzk}$
$u_y = y_k = \alpha_{yxk} x_0 + \alpha_{yyk} y_0 + \alpha_{yzk} z_{w0}$
$u_y{}'(x_0) = \alpha_{yxk}$
$u_y{}'(y_0) = \alpha_{yyk}$
$u_y{}'(z_{w0}) = \alpha_{yzk}$
$v_z = z_k = z_{\text{lens}} - \left(h - \frac{h - (\alpha_{zxk} x_0 + \alpha_{zyk} y_0 + \alpha_{zzk} z_{w0})}{n} \right)$
$v_z{}'(x_0) = -\alpha_{zxk}/n$
$v_z{}'(y_0) = -\alpha_{zyk}/n$
$v_z{}'(z_{w0}) = -\alpha_{zzk}/n$

$$\frac{\partial}{\partial x_0} \left(\frac{x_k}{z_k} \right) = \frac{u_x{}' v_z - u_x v_z{}'}{v^2} = \frac{\alpha_{xxk} z_k + \alpha_{zxk} x_k / n}{{z_k}^2} \tag{26}$$

$$\frac{\partial}{\partial y_0} \left(\frac{x_k}{z_k} \right) = \frac{\alpha_{xyk} z_k + \alpha_{zyk} x_k / n}{{z_k}^2} \tag{27}$$

$$\frac{\partial}{\partial z_{w0}} \left(\frac{x_k}{z_k} \right) = \frac{\alpha_{xzk} z_k + \alpha_{zzk} x_k / n}{{z_k}^2} \tag{28}$$

$$\frac{\partial}{\partial x_0} \left(\frac{y_k}{z_k} \right) = \frac{u_y{}' v_z - u_y v_z{}'}{v^2} = \frac{\alpha_{yxk} z_k + \alpha_{zxk} y_k / n}{{z_k}^2} \tag{29}$$

$$\frac{\partial}{\partial y_0} \left(\frac{y_k}{z_k} \right) = \frac{\alpha_{yyk} z_k + \alpha_{zyk} y_k / n}{{z_k}^2} \tag{30}$$

$$\frac{\partial}{\partial z_{w0}} \left(\frac{y_k}{z_k} \right) = \frac{\alpha_{yzk} z_k + \alpha_{zzk} y_k / n}{{z_k}^2} \tag{31}$$

$$\frac{\partial}{\partial x_0} \left(\left(\frac{x_k}{z_k} \right)^2 \right) = 2 \frac{x_k}{z_k} \frac{\partial}{\partial x_0} \left(\frac{x_k}{z_k} \right) \tag{32}$$

$$\frac{\partial}{\partial y_0} \left(\left(\frac{x_k}{z_k} \right)^2 \right) = 2 \frac{x_k}{z_k} \frac{\partial}{\partial y_0} \left(\frac{x_k}{z_k} \right) \tag{33}$$

$$\frac{\partial}{\partial z_{w0}} \left(\left(\frac{x_k}{z_k} \right)^2 \right) = 2 \frac{x_k}{z_k} \frac{\partial}{\partial z_{w0}} \left(\frac{x_k}{z_k} \right) \tag{34}$$

$$\frac{\partial}{\partial x_0} \left(\left(\frac{y_k}{z_k} \right)^2 \right) = 2 \frac{y_k}{z_k} \frac{\partial}{\partial x_0} \left(\frac{y_k}{z_k} \right) \tag{35}$$

$$\frac{\partial}{\partial y_0}\left(\left(\frac{y_k}{z_k}\right)^2\right) = 2\frac{y_k}{z_k}\frac{\partial}{\partial y_0}\left(\frac{y_k}{z_k}\right) \tag{36}$$

$$\frac{\partial}{\partial z_{w0}}\left(\left(\frac{y_k}{z_k}\right)^2\right) = 2\frac{y_k}{z_k}\frac{\partial}{\partial z_{w0}}\left(\frac{y_k}{z_k}\right) \tag{37}$$

$$\sigma_k = a\frac{AS_2}{S_1}\frac{|S_1 - z_k|}{z_k} \tag{38}$$

$$\frac{|S_1 - z_k|}{z_k} = \frac{|S_1 - z_{\text{lens}} - \left(h - \frac{h-(\alpha_{zxk}x_0 + \alpha_{zyk}y_0 + \alpha_{zzk}z_{w0})}{n}\right)|}{z_{\text{lens}} - \left(h - \frac{h-(\alpha_{zxk}x_0 + \alpha_{zyk}y_0 + \alpha_{zzk}z_{w0})}{n}\right)}$$

$$u = S_1 - z_k = S_1 - z_{\text{lens}} - \left(h - \frac{h-(\alpha_{zxk}x_0 + \alpha_{zyk}y_0 + \alpha_{zzk}z_{w0})}{n}\right)$$

$$\frac{\partial \sigma_k}{\partial x_0} = a\frac{AS_2}{S_1}\frac{\partial}{\partial x_0}\frac{|S_1 - z_k|}{z_k} = a\frac{AS_2}{S_1}\frac{\alpha_{zxk}sign(u)z_k/n - |u|(-\alpha_{zxk}/n)}{{z_k}^2} = a\frac{AS_2}{S_1}\frac{\alpha_{zxk}sign(u)z_k/n + \alpha_{zxk}|u|/n}{{z_k}^2} \tag{39}$$

$$\frac{\partial \sigma_k}{\partial y_0} = a\frac{AS_2}{S_1}\frac{\partial}{\partial y_0}\frac{|S_1 - z_k|}{z_k} = a\frac{AS_2}{S_1}\frac{\alpha_{zyk}sign(u)z_k/n + \alpha_{zyk}|u|/n}{{z_k}^2} \tag{40}$$

$$\frac{\partial \sigma_k}{\partial z_{w0}} = a\frac{AS_2}{S_1}\frac{\partial}{\partial z_{w0}}\frac{|S_1 - z_k|}{z_k} = a\frac{AS_2}{S_1}\frac{\alpha_{zzk}sign(u)z_k/n + \alpha_{zzk}|u|/n}{{z_k}^2} \tag{41}$$

$$Q = \sum_i \sum_k r_{ik}\left[\log\pi_k - \log(2\pi{\sigma_k}^2) - \frac{{\sigma_k}^{-2}}{2}(\boldsymbol{t_i} - \boldsymbol{\mu_k})^T(\boldsymbol{t_i} - \boldsymbol{\mu_k})\right] \tag{42}$$

$$= \sum_i \sum_k r_{ik}\left[\log\pi_k - \log(2\pi{\sigma_k}^2) - \frac{{\sigma_k}^{-2}}{2}\left({t_{ix}}^2 - 2t_{ix}S_2\frac{x_k}{z_k} + {S_2}^2\left(\frac{x_k}{z_k}\right)^2 + {t_{iy}}^2 - 2t_{iy}S_2\frac{y_k}{z_k} + {S_2}^2\left(\frac{y_k}{z_k}\right)^2\right)\right] \tag{43}$$

$$f(x_k, y_k, z_k) = \left({t_{ix}}^2 - 2t_{ix}S_2\frac{x_k}{z_k} + {S_2}^2\left(\frac{x_k}{z_k}\right)^2 + {t_{iy}}^2 - 2t_{iy}S_2\frac{y_k}{z_k} + {S_2}^2\left(\frac{y_k}{z_k}\right)^2\right) \tag{44}$$

$$\frac{\partial f}{\partial x_0} = -2t_{ix}S_2\frac{\partial}{\partial x_0}\left(\frac{x_k}{z_k}\right) + {S_2}^2\frac{\partial}{\partial x_0}\left(\left(\frac{x_k}{z_k}\right)^2\right) - 2t_{iy}S_2\frac{\partial}{\partial x_0}\left(\frac{y_k}{z_k}\right) + {S_2}^2\frac{\partial}{\partial x_0}\left(\left(\frac{y_k}{z_k}\right)^2\right) \tag{45}$$

$$\frac{\partial f}{\partial y_0} = -2t_{ix}S_2\frac{\partial}{\partial y_0}\left(\frac{x_k}{z_k}\right) + {S_2}^2\frac{\partial}{\partial y_0}\left(\left(\frac{x_k}{z_k}\right)^2\right) - 2t_{iy}S_2\frac{\partial}{\partial y_0}\left(\frac{y_k}{z_k}\right) + {S_2}^2\frac{\partial}{\partial y_0}\left(\left(\frac{y_k}{z_k}\right)^2\right) \tag{46}$$

$$\frac{\partial f}{\partial z_{w0}} = -2t_{ix}S_2\frac{\partial}{\partial z_{w0}}\left(\frac{x_k}{z_k}\right) + {S_2}^2\frac{\partial}{\partial z_{w0}}\left(\left(\frac{x_k}{z_k}\right)^2\right) - 2t_{iy}S_2\frac{\partial}{\partial z_{w0}}\left(\frac{y_k}{z_k}\right) + {S_2}^2\frac{\partial}{\partial z_{w0}}\left(\left(\frac{y_k}{z_k}\right)^2\right) \tag{47}$$

$$\frac{\partial Q}{\partial x_0} = \sum_i \sum_k r_{ik}\left[-2{\sigma_k}^{-1}\frac{\partial \sigma_k}{\partial x_0} - \left(-{\sigma_k}^{-3}\frac{\partial \sigma_k}{\partial x_0}f + \frac{{\sigma_k}^{-2}}{2}\frac{\partial f}{\partial x_0}\right)\right] \tag{48}$$

$$\frac{\partial Q}{\partial y_0} = \sum_i \sum_k r_{ik} \left[-2{\sigma_k}^{-1} \frac{\partial \sigma_k}{\partial y_0} - \left(-{\sigma_k}^{-3} \frac{\partial \sigma_k}{\partial y_0} f + \frac{{\sigma_k}^{-2}}{2} \frac{\partial f}{\partial y_0} \right) \right] \tag{49}$$

$$\frac{\partial Q}{\partial z_{w0}} = \sum_i \sum_k r_{ik} \left[-2{\sigma_k}^{-1} \frac{\partial \sigma_k}{\partial z_{w0}} - \left(-{\sigma_k}^{-3} \frac{\partial \sigma_k}{\partial z_{w0}} f + \frac{{\sigma_k}^{-2}}{2} \frac{\partial f}{\partial z_{w0}} \right) \right] \tag{50}$$

I.2. Weighted Likelihood

w_i is the weight assigned to photon sample i. $w_i = \sum_{j \in S_i^q} \exp\left(-\frac{||\boldsymbol{t_i} - \boldsymbol{t_j}||_2^2}{\nu} \right)$ where S_i^q is the set of q nearest neighbors of photon i, and ν is a positive scalar.

$$L(\boldsymbol{\theta}; \boldsymbol{t}, \boldsymbol{z}) = \prod_{i=1}^{N} \prod_{k=0}^{K} \left[\pi_k \mathcal{N}(\boldsymbol{t_i}; \boldsymbol{\mu_k}, \frac{1}{w_i} \sigma_k^2) \right]^{\mathbb{1}(z_i = k)} \tag{51}$$

$$= \prod_{i=1}^{N} \prod_{k=0}^{K} \left[\pi_k \frac{w_i}{2\pi {\sigma_k}^2} \exp\left(-\frac{w_i}{2{\sigma_k}^2} (\boldsymbol{t_i} - \boldsymbol{\mu_k})^T (\boldsymbol{t_i} - \boldsymbol{\mu_k}) \right) \right]^{\mathbb{1}(z_i = k)} \tag{52}$$

$$Q = \sum_i \sum_k r_{ik} \left[\log(\pi_k) + \log(w_i) - \log(2\pi {\sigma_k}^2) - \frac{w_i {\sigma_k}^{-2}}{2} (\boldsymbol{t_i} - \boldsymbol{\mu_k})^T (\boldsymbol{t_i} - \boldsymbol{\mu_k}) \right] \tag{53}$$

$$\frac{\partial Q}{\partial x_0} = \sum_i \sum_k r_{ik} \left[-2{\sigma_k}^{-1} \frac{\partial \sigma_k}{\partial x_0} - w_i \left(-{\sigma_k}^{-3} \frac{\partial \sigma_k}{\partial x_0} f + \frac{{\sigma_k}^{-2}}{2} \frac{\partial f}{\partial x_0} \right) \right] \tag{54}$$

$$\frac{\partial Q}{\partial y_0} = \sum_i \sum_k r_{ik} \left[-2{\sigma_k}^{-1} \frac{\partial \sigma_k}{\partial y_0} - w_i \left(-{\sigma_k}^{-3} \frac{\partial \sigma_k}{\partial y_0} f + \frac{{\sigma_k}^{-2}}{2} \frac{\partial f}{\partial y_0} \right) \right] \tag{55}$$

$$\frac{\partial Q}{\partial z_{w0}} = \sum_i \sum_k r_{ik} \left[-2{\sigma_k}^{-1} \frac{\partial \sigma_k}{\partial z_{w0}} - w_i \left(-{\sigma_k}^{-3} \frac{\partial \sigma_k}{\partial z_{w0}} f + \frac{{\sigma_k}^{-2}}{2} \frac{\partial f}{\partial z_{w0}} \right) \right] \tag{56}$$

I.3. Regularized Objective

Regularized objective function R, where $\boldsymbol{\mu_k^0}$ is the centroid obtained from the initialization procedure corresponding to event/mirror reflection k.

$$R = Q - \lambda \sum_{k=0}^{K} \left\| \boldsymbol{\mu_k} - \boldsymbol{\mu_k^0} \right\|_2^2 \tag{57}$$

$$g_k = \left\| \boldsymbol{\mu_k} - \boldsymbol{\mu_k^0} \right\|_2^2 = (\mu_{kx} - \mu_{kx}^0)^2 + (\mu_{ky} - \mu_{ky}^0)^2 = \left(\left(S_2 \frac{x_k}{z_k} \right) - \mu_{kx}^0 \right)^2 + \left(\left(S_2 \frac{y_k}{z_k} \right) - \mu_{ky}^0 \right)^2 \tag{58}$$

$$\frac{\partial g_k}{\partial x_0} = 2 \left(S_2 \frac{x_k}{z_k} - \mu_{kx}^0 \right) \left(S_2 \frac{\partial}{\partial x_0} \left(\frac{x_k}{z_k} \right) \right) + 2 \left(S_2 \frac{y_k}{z_k} - \mu_{ky}^0 \right) \left(S_2 \frac{\partial}{\partial x_0} \left(\frac{y_k}{z_k} \right) \right) \tag{59}$$

$$\frac{\partial g_k}{\partial y_0} = 2\left(S_2\frac{x_k}{z_k} - \mu_{kx}^0\right)\left(S_2\frac{\partial}{\partial y_0}\left(\frac{x_k}{z_k}\right)\right) + 2\left(S_2\frac{y_k}{z_k} - \mu_{ky}^0\right)\left(S_2\frac{\partial}{\partial y_0}\left(\frac{y_k}{z_k}\right)\right) \tag{60}$$

$$\frac{\partial g_k}{\partial z_{w0}} = 2\left(S_2\frac{x_k}{z_k} - \mu_{kx}^0\right)\left(S_2\frac{\partial}{\partial z_{w0}}\left(\frac{x_k}{z_k}\right)\right) + 2\left(S_2\frac{y_k}{z_k} - \mu_{ky}^0\right)\left(S_2\frac{\partial}{\partial z_{w0}}\left(\frac{y_k}{z_k}\right)\right) \tag{61}$$

$$\frac{\partial R}{\partial x_0} = \frac{\partial Q}{\partial x_0} - \lambda\sum_{k=0}^{K}\frac{\partial g_k}{\partial x_0} \tag{62}$$

$$\frac{\partial R}{\partial y_0} = \frac{\partial Q}{\partial y_0} - \lambda\sum_{k=0}^{K}\frac{\partial g_k}{\partial y_0} \tag{63}$$

$$\frac{\partial R}{\partial z_{w0}} = \frac{\partial Q}{\partial z_{w0}} - \lambda\sum_{k=0}^{K}\frac{\partial g_k}{\partial z_{w0}} \tag{64}$$